Photodiagnosis and Photodynamic Therapy 25 (2019) 309–316

Contents lists available at ScienceDirect

Photodiagnosis and Photodynamic Therapy

journal homepage: www.elsevier.com/locate/pdpdt

Expression of peptide transporter 1 has a positive correlation in protoporphyrin IX accumulation induced by 5-aminolevulinic acid with photodynamic detection of non-small cell lung cancer and metastatic brain tumor specimens originating from non-small cell lung cancer

Koji Omoto[a], Ryosuke Matsuda[a,*], Yasushi Nakai[b], Yoshihiro Tatsumi[b], Tsutomu Nakazawa[a,c], Yoshitaka Tanaka[a], Yoichi Shida[a], Toshiharu Murakami[a], Fumihiko Nishimura[a], Ichiro Nakagawa[a], Yasushi Motoyama[a], Mitsutoshi Nakamura[a], Kiyohide Fujimoto[b], Nakase Hiroyuki[a]

[a] Department of Neurosurgery, Nara Medical University, Kashihara, Nara, Japan
[b] Department of Urology, Nara Medical University, Kashihara, Nara, Japan
[c] Grandsoul Research Institute for Immunology, Inc., Uda, Nara, Japan

ARTICLE INFO

Keywords:
Protoporphyrin IX
Peptide transporter 1
Non-small lung cancer
Brain
Metastasis

ABSTRACT

Background: Recently, 5-aminolevulinic acid (5-ALA)-induced protoporphyrin IX fluorescence was reported to be a useful tool during total surgical resection of high-grade gliomas. However, the labeling efficacy of protoporphyrin IX fluorescence is lower in metastatic brain tumors compared to that in high-grade gliomas, and the mechanism underlying protoporphyrin IX fluorescence in metastatic brain tumors remains unclear. Lung cancer, particularly non-small cell lung cancer (NSCLC), is the most common origin for metastatic brain tumor. Therefore, we investigated the mechanism of protoporphyrin IX fluorescence in NSCLC and associated metastatic brain tumors.

Methods: Western blotting and quantitative real-time polymerase chain reaction (qRT-PCR) was employed to evaluate the protein and mRNA levels of five transporters and enzymes involved in the porphyrin biosynthesis pathway: peptide transporter 1 (PEPT1), hydroxymethylbilane synthase (HMBS), ferrochelatase (FECH), ATP-binding cassette 2 (ABCG2), and heme oxygenase 1 (HO-1). The correlation between protein, mRNA, and protoporphyrin IX levels in NSCLC cells were evaluated *in vitro*. Immunohistochemistry was used to determine proteins that played a key role in intraoperative protoporphyrin IX fluorescence in clinical samples from patients with NSCLC and pathologically confirmed metastatic brain tumors.

Results: A significant correlation between PEPT1 expression and protoporphyrin IX accumulation *in vitro* was identified by western blotting ($P = 0.003$) and qRT-PCR ($P = 0.04$). Immunohistochemistry results indicated that there was a significant difference in PEPT1 between the intraoperative protoporphyrin IX fluorescence-positive and protoporphyrin IX fluorescence-negative groups ($P = 0.009$).

Conclusion: Expression of PEPT1 was found to be positively correlated with 5-ALA-induced protoporphyrin IX accumulation detected by photodynamic reaction in metastatic brain tumors originating from NSCLC.

1. Introduction

Metastatic brain tumors are the most common cerebral neoplasms with an increasing incidence [1]. Surgical resection of single cerebral metastatic lesions is a key element of multimodal therapy, and the surgical standard is a microsurgical, white-light, microscope-assisted circumferential stripping of the tumor from the adjacent brain tissue [2]. The primary aim of the treatment is to achieve local tumor control through complete surgical resection with low morbidity and mortality. Cerebral metastases with an infiltrative growth pattern and small tumor remnants after planned total resection are implicated as reasons for the high local recurrence rate [3,4]. Fluorescence-guided resection is a widely used clinical approach, especially during surgery for glioblastoma [5] and bladder cancer [6], which can identify precise tumor

* Corresponding author at: Department of Neurosurgery, Nara Medical University, 840 Shijo-cho, Kashihara, 634-8522, Nara, Japan.
E-mail address: cak93500@pop02.odn.ne.jp (R. Matsuda).

https://doi.org/10.1016/j.pdpdt.2019.01.009
Received 1 October 2018; Received in revised form 11 December 2018; Accepted 7 January 2019
Available online 11 January 2019
1572-1000/

margins and prevent oversight of small lesions that are otherwise invisible. Stummer et al. [5] demonstrated that this surgical technique facilitated more complete resection of contrast-enhancing lesions compared with conventional microsurgery and improved progression-free survival in patients with glioblastoma. Utilization of this technique for metastatic brain tumors has been presented as an option to visualize residual tumor tissue and maximize the extent of surgical resection [7].

5-aminolevulinic acid (5-ALA) is a precursor of heme biosynthesis that is converted to the active photosensitizer protoporphyrin IX in cells [8,9]. As protoporphyrin IX preferentially accumulates in malignant tissues [10], exogenous administration of 5-ALA enables the detection of tumors that exhibit enhanced protoporphyrin IX fluorescence after blue-light illumination. 5-ALA positivity in metastatic brain tumors depends on the primary cancer and pathological diagnosis and ranges between 12.5% and 100% [11], which is lower than its detection rate in high-grade glioma. However, protoporphyrin IX fluorescence remains unsatisfactory for the diagnosis of metastatic brain tumors that accumulate insufficient protoporphyrin IX levels [12,13]. Although the mechanism underlying protoporphyrin IX accumulation in glioblastoma was reported [14–18], the mechanism in other brain tumors, specifically metastatic brain tumors, remains unclear. Lung cancer, especially non-small cell lung cancer (NSCLC), is the most common origin for metastatic brain tumors. Therefore, we investigated the mechanism of protoporphyrin IX fluorescence in NSCLC and metastatic brain tumors originating from NSCLC.

Successful protoporphyrin IX accumulation in the porphyrin biosynthesis pathway rely on the activity of enzymes that synthesize and metabolize protoporphyrin IX as well as the activity of 5-ALA transporters [19]. Previous studies reported the presence of distinct enzymes and transporters of the porphyrin biosynthesis pathway in various malignant tumors. Peptide transporter 1 (PEPT1) is an oligopeptide transporter that uptakes 5-ALA into cells from the extracellular medium, and increased PEPT1 levels are associated with increased protoporphyrin IX accumulation in gastric cancer [20] and bladder cancer cells [21]. Conversely, hydroxymethylbilane synthase (HMBS) catalyzes porphobilinogen into hydroxymethylbilane, and increased HMBS expression increases protoporphyrin IX accumulation in bladder cancer cells [22]. ATP-binding cassette 2 (ABCG2) transports protoporphyrin IX across the mitochondrial and plasma membranes, and its suppression was shown to increase protoporphyrin IX accumulation in glioblastoma [16] and urothelial cancer [20,21]. Recently, heme oxygenase 1 (HO-1), a heme-degrading enzyme, was reported to be further upregulated following treatment with 5-ALA in glioma cells [18], whereas siRNA knockdown of *HO-1* reduced protoporphyrin IX accumulation in urothelial cancer cells [22]. Ferrochelatase (FECH) is located in the inner mitochondrial membrane and encodes a key enzyme that catalyzes the conversion of protoporphyrin IX to heme; suppressed expression of FECH was demonstrated to increase protoporphyrin IX accumulation in glioblastoma and bladder cancer [10,14,22,23].

We hypothesized that NSCLC might exhibit distinct gene and protein expression patterns associated with activated enzymes and/or transporters in the porphyrin biosynthesis pathway and that these changes might be represented in changes in protoporphyrin IX fluorescence intensity in NSCLC and associated metastatic brain tumors.

2. Materials and methods

2.1. Cell culture

The human NSCLC cell lines RERF-LC-KJ and LK-2 were provided by the Grandsoul Research Institute for Immunology (Uda, Nara, Japan). The following cell lines were provided by RIKEN (BRC through the National Bio-Resource Project of the MEXT, Japan): A549, LC-1/sq, RERF-LC-AI, and HLC-1. A549, RERF-LC-KJ, and LC-1/sq are squamous cell carcinoma cell lines, whereas LK-2, RERF-LC-AI, and HLC-1 are adenocarcinoma cell lines. Cells were maintained under 5% CO_2 at 37 °C in Dulbecco's modified Eagle's medium (Life Technologies, Tokyo, Japan) supplemented with 10% fetal bovine serum, 100 U/ml penicillin, and 100 μg/ml streptomycin (Life Technologies, Tokyo, Japan)

2.2. Photodynamic detection of protoporphyrin IX in NSCLC cell lines

A total of 5.0×10^5 cells were treated with 1 mM 5-ALA diluted in phosphate-buffered saline (PBS) or PBS alone. The samples were then incubated at 37 °C for 2 h. After centrifugation at 1500 rpm for 5 min, the supernatants were removed, and the pellets were resuspended in 40 μl PBS. Next, 20 μl of the resuspended cells and 20 μl protoporphyrin IX (Sigma Aldrich, St. Louis, MO, USA) from a 1-mg/μl stock in PBS were pipetted into each well of a 96-well plate. The fluorescence intensity of samples was measured using a spectrophotometer (Infinite 200 pro®; Tecan, Männendorf, Switzerland) with the appropriate settings (excitation wavelength, 405 nm; emission wavelength, 550–700 nm; gain 160), and peak fluorescence intensity at 635 nm was measured. Intracellular protoporphyrin IX accumulation in all cell lines was reported as the measured fluorescence intensity normalized to the protoporphyrin IX quantity per 10,000 cells. Specifically, the difference between the intensity of the 5-ALA-treated sample and that of the non-treated sample at 635 nm was divided by the intensity of protoporphyrin IX, as described previously [23].

2.3. Western blotting

Total protein was extracted using lysis buffer (200 mM-Tris HCL, 8% SDS, 40% Glycerol, 1% BPB and β-mercaptoethanol) supplemented with protease inhibitors. Protein concentrations were quantified using the Pierce™ BCA protein assay kit (Thermo Fisher Scientific, Yokohama, Japan). The proteins were heated at 95 °C for 5 min and electrophoresed in 5%–20% sodium dodecyl sulfate-polyacrylamide gels (Wako Pure Chemical Industries, Osaka, Japan). Gels were transferred to polyvinylidene difluoride membranes at 15 V for 30 min. After blocking in Tris-buffered saline containing 5% skim milk and 0.1% Tween-20 for 1 h, the membranes were incubated with primary antibodies overnight at 4 °C. The primary antibodies used in this study were as follows: rabbit polyclonal anti-PEPT1 (1:500 dilution; Santa Cruz Biotechnology, Dallas, Texas, USA), rabbit polyclonal anti-HMBS (1:200 dilution; Sigma Aldrich), rabbit monoclonal anti-ABCG2 (1:1000 dilution; Cell Signaling Technology, Danvers, MA, USA), mouse monoclonal anti－HO-1 (1:500 dilution; BD transduction Laboratories, San Diego, CA, USA), rabbit polyclonal anti-FECH (1:500 dilution; Bioss Antibodies, Woburn, Massachusetts, USA), and mouse monoclonal anti-actin antibody (1:50,000 dilution, Sigma Aldrich). Next, the membranes were incubated with secondary antibodies conjugated to horseradish peroxidase for 1 h at room temperature. The bound secondary antibodies were visualized using an enhanced chemiluminescence kit (ECL Plus western blotting detection system, GE Healthcare). Band densities were quantified using ImageJ (National Institutes of Health, Bethesda, Maryland, USA), and relative proteins amounts were normalized to actin bands.

2.4. Quantitative real-time polymerase chain reaction

MicroRNAs were extracted from each cell line using the RNeasy mini kit (QIAGEN, Hilden, Germany) according to the manufacturer's instructions. Briefly, first-strand cDNA was synthesized from the extracted mRNA in a reverse transcriptase reaction using the Primerscript RT reagent kit (TaKaRa Bio, Shiga, Japan). Quantitative real-time polymerase chain reaction (qRT-PCR) was performed using the synthesized cDNA preparations to detect mRNA levels of *PEPT1*, *HMBS*, *ABCG2*, *HO-1*, and *FECH*. *GAPDH* was used for quantification (Thermo Fisher Scientific), and the Taqman assay was used for the reactions. The reaction conditions were as follows: denaturation, 95 °C for 10 min; amplification and quantification, 95 °C for 15 s and 60 °C for 60 s, for 45

cycles. The data were analyzed using the Light Cycler Data Analysis software. Relative mRNA levels were calculated as the ratio of the target mRNA level to *GAPDH* mRNA level.

2.5. Metastatic brain tumor samples

This study included retrospectively collected brain tumor samples from ten patients diagnosed with metastatic brain tumor originated from NSCLC at Nara Medical University between January 2009 and March 2017. All ten patients with large metastatic brain tumors from NSCLC underwent surgical resection under 5-ALA-guided surgery. Large metastatic brain tumor was defined as a lesion larger than 30 mm, and maximum diameter was based on the axial, coronal, or sagittal image by gadolinium-enhanced magnetic resonance. Three hours prior to the surgery, patients were orally administered 20 mg/kg 5-ALA (Cosmo Bio, Tokyo, Japan). After the brain tumor bulk was exposed, protoporphyrin IX fluorescence was visualized with an operating microscope (OPMI-Pentero; Carl Zeiss, Jena, Germany). The target region was exposed to blue light with a peak wavelength of 405 nm, and protoporphyrin IX fluorescence was measured at 630 nm with an optical filter. The tumor fluorescence was independently evaluated as positive or negative by two neurosurgeons to ensure the objectivity of fluorescence measurements. After tumor resection, the samples were fixed with 10% formalin and embedded in paraffin for histological diagnosis and immunohistochemistry.

The protocols for the pathological specimens, storage, and measurements required for the present study were approved by the Ethics Committee at Nara Medical University (Approval No. 1238). This clinical study was conducted according to the principles of the Declaration of Helsinki. Informed consent was obtained from all patients.

2.6. Immunohistochemistry

The paraffin sections were routinely deparaffinized and rehydrated. For deparaffinization, the sections were incubated three times in xylene, 3 min each time. For rehydration, the sections were incubated twice in 100% ethanol for 3 min each time, twice in 95% ethanol for 3 min each time, and once in distilled PBS. For each patient, after rehydration, one sample section was stained with hematoxylin & eosin, and the other section was autoclaved, and stained subsequently using the streptavidin-biotin method with the Histofine SAB-PO kit (Nichirei, Tokyo, Japan) according to the manufacturer's instructions. Specificity of the antibodies were determined by control slides that were concomitantly stained with secondary antibody only.

The primary antibodies and incubation conditions were as follows: rabbit polyclonal anti-PEPT1 (1:200 dilution; Santa Cruz Biotechnology), rabbit polyclonal anti-HMBS (1:500 dilution; Sigma Aldrich), rabbit monoclonal anti-ABCG2 (1:350 dilution; Cell Signaling Technology), mouse monoclonal anti－HO-1 (1:200 dilution; BD Transduction Laboratories), and rabbit polyclonal anti-FECH (1:500 dilution; Bioss Antibodies), incubated overnight at 4 ˚C; mouse monoclonal anti-Ki-67 (clone MIB-1; 1:250 dilution; Santa Cruz Biotechnology) at room temperature for 1 h. The antibody staining intensities were evaluated as the percentage of stained cells among all cells in five high-power fields for each case. For Ki-67 staining, cells with the stained nuclei were counted as positive. For PEPT1, HMBS, ABCG2, HO-1, and FECH, cells with stained cytoplasm were counted as positive. Two investigators, both of whom were blinded to the patient data, evaluated the percentage of stained tumor cells. A third investigator reviewed discrepancies and rendered final judgment.

2.7. Statistical analysis

Statistical analysis was performed with SPSS for Windows (version 20.0; IBM, Armonk, USA). Pearson's correlation analysis was used to determine the degree of correlation between two variables by western blotting and qRT-PCR. The Mann-Whitney *U* test was used to analyze differences between two continuous variables for immunohistochemistry. P values < 0.05 were considered statistically significant.

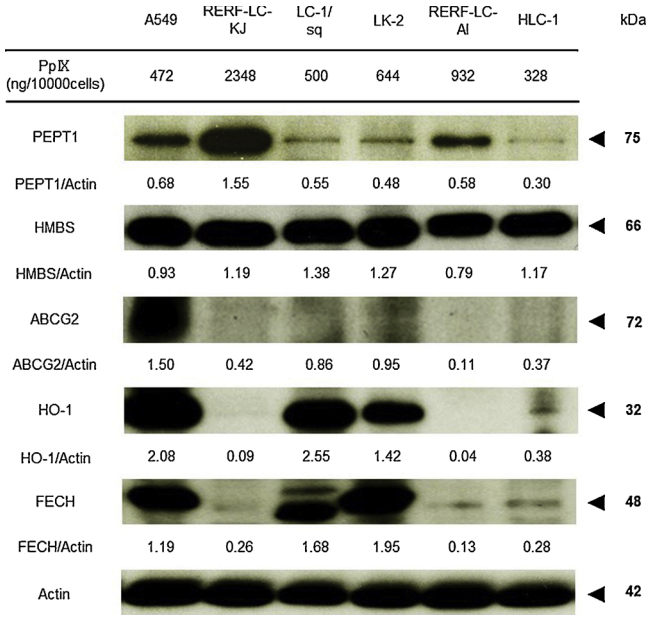

Fig. 1. The account of intracellular protoporphyrin IX accumulation of each cell lines translated by fluorescence intensity at the top, and the expression of each protein on western blotting, the relative amounts of proteins normalized to actin bands.
PEPT1: peptide transporter1, HMBS: hydroxymethylbilane synthase, ABCG2: ATP-binding cassette group2, HO-1: heme oxygenase-1, FECH: ferrochelatase.

3. Results

3.1. Photodynamic detection of protoporphyrin IX in NSCLC cell lines

The fluorescence intensities expressed as the among of intracellular protoporphyrin IX per cell were 472, 2348, 500, 644, 932, and 328 ng/10,000 cells for A549, RERF-LC-KJ, LC-1/sq, LK-2, RERF-LC-AI, and HLC-1 cells, respectively (Fig. 1).

3.2. PEPT1 protein level is associated with protoporphyrin IX accumulation in NSCLC cells

The results of western blotting for PEPT1, HMBS, ABCG2, HO-1, FECH, and actin are shown in Fig. 1. The correlation between the protein levels and intracellular protoporphyrin IX accumulation in each cell line, which was evaluated using ImageJ, is shown in Fig. 2. Briefly, a significant correlation was observed between the PEPT1 protein level and protoporphyrin IX accumulation ($P = 0.003$, $r = 0.95$; Fig. 2)

3.3. PEPT1 mRNA expression is associated with protoporphyrin IX accumulation in NSCLC cells

The correlation between the relative mRNA levels for each cell line and intracellular protoporphyrin IX accumulation is shown in Fig. 3. In summary, a significant correlation was observed between *PEPT1* mRNA expression and protoporphyrin IX accumulation, similar to the western blotting results ($P = 0.04$, $r = 0.82$; Fig. 3)

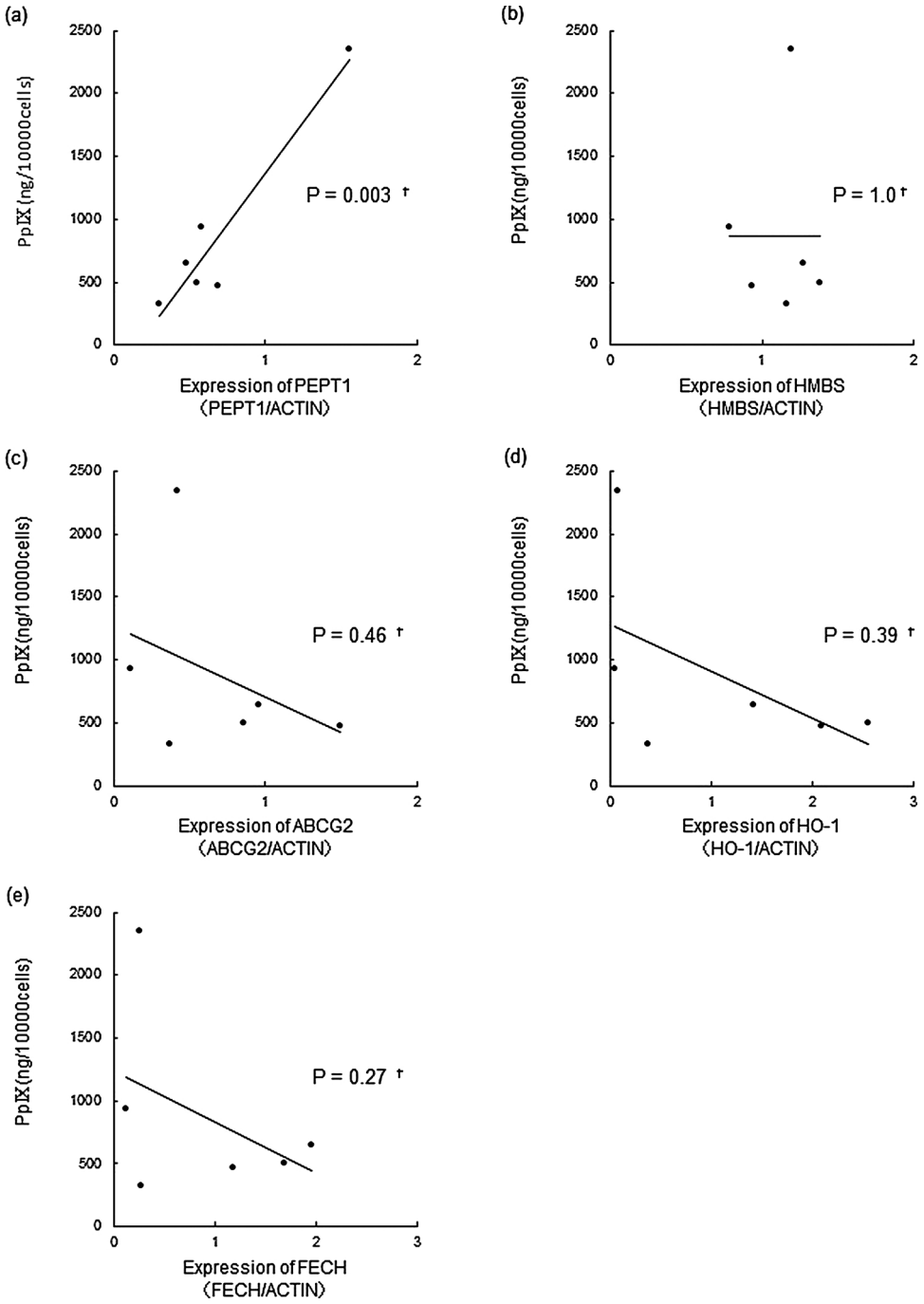

Fig. 2. Correlation between the expression of each protein by WB and the account of intracellular protoporphyrin IX accumulation of each cell lines.
(a) PEPT1: peptide transporter1, (b) HMBS: hydroxymethylbilane synthase, (c) ABCG2: ATP-binding cassette group2, (d) HO-1: heme oxygenase-1, (e) FECH: ferrochelatase.

3.4. Characteristics of the cohort of patients with metastatic brain tumors originating from NSCLC who underwent 5-ALA-guided surgery

Of the ten patients with metastatic brain tumors originating from NSCLC, the intraoperative protoporphyrin IX fluorescence during surgery was positive for five patients and negative for the remaining five patients. The details of the pathological diagnosis of the patient cohort are provided in Table 1. Briefly, NSCLC cases included adenocarcinoma, adenosquamous carcinoma, spindle cell carcinoma, and giant cell carcinoma. Only four patients underwent pulmonary lobectomy for NSCLC.

3.5. Immunohistochemistry

The patient cohort was divided into the 5-ALA-positive and 5-ALA-negative groups, and the percentages of cells positive for PEPT1, HMBS, ABCG2, HO-1, FECH, and Ki-67 were measured in all specimens. In agreement with the western blotting and qRT-PCR results, the percentage of PEPT1-positive cells was significantly higher in the 5-ALA-positive group compared with the 5-ALA-negative group ($P = 0.009$) (Fig. 4). Specimens from two cases, one 5-ALA-positive and one 5-ALA-negative case, that were stained with PEPT1 are shown in Fig. 5. For three of the 5-ALA positive patients, the primary lung tumor was

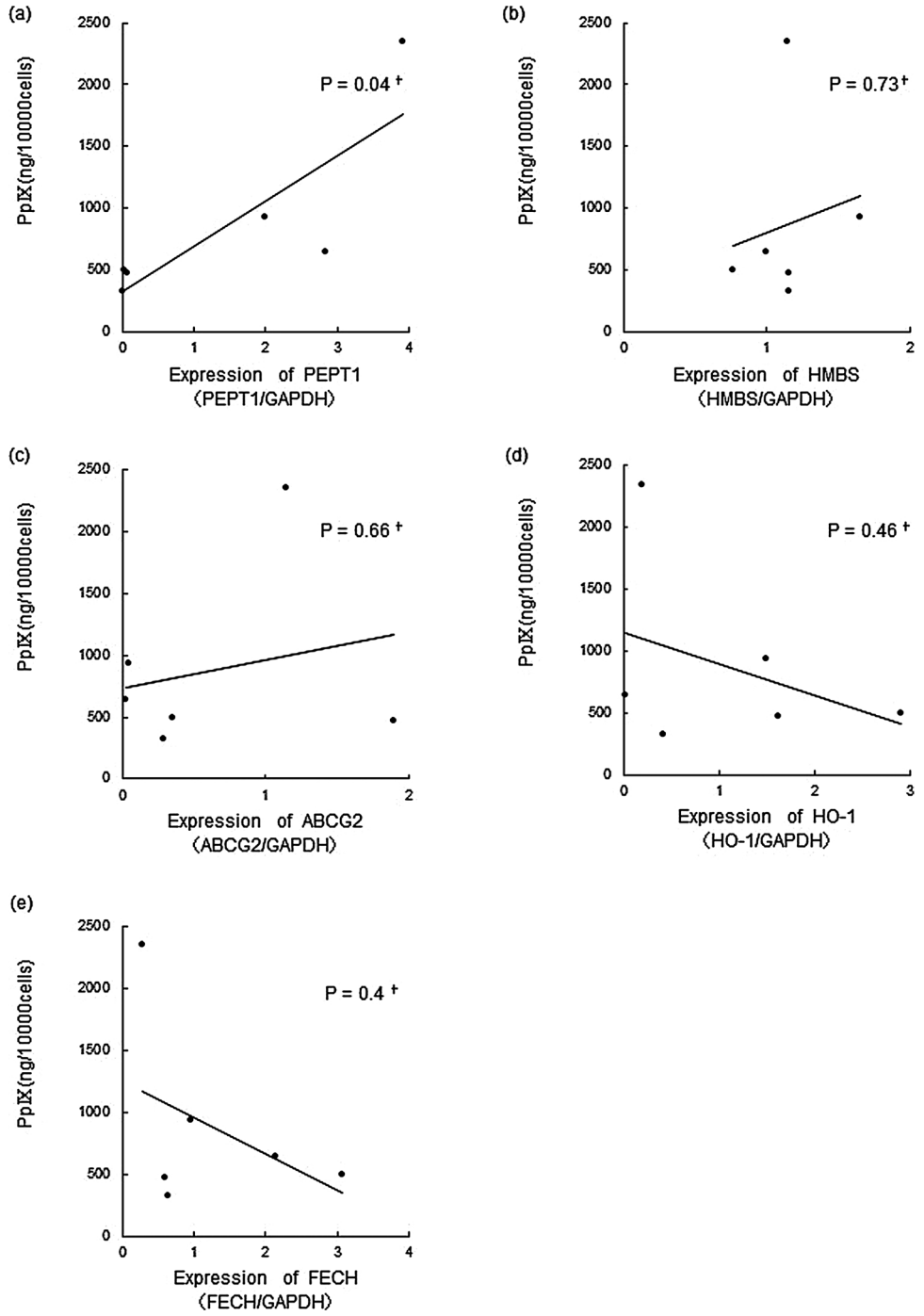

Fig. 3. Correlation between the expression of each mRNA by QRT-PCR and the account of intracellular protoporphyrin IX accumulation of each cell lines.
(a) PEPT1: peptide transporter1, (b) HMBS: hydroxymethylbilane synthase, (c) ABCG2: ATP-binding cassette group2, (d) HO-1: heme oxygenase-1, (e) FECH: ferrochelatase.

surgically removed before the diagnosis of the brain metastasis. The primary lung specimens were stained for PEPT1 using the same immunohistochemistry method, which revealed that the percentage of PEPT1-positive cells was also high in the primary lesion (Fig. 6), which was not statistically significant because of the small number of cases.

4. Discussion

4.1. 5-ALA fluorescence in metastatic brain tumor specimens

The main finding of the current study was that PEPT1 was strongly correlated with protoporphyrin IX fluorescence in metastatic brain tumors originating from NSCLC *in vitro* and in clinical samples. Kamp et al. [12] reported that the absence of protoporphyrin IX fluorescence in surgically removed metastatic brain tumors might be a risk factor for local progression. Additionally, Marbacher et al. [11] reported that 5-ALA was a promising tool for improving intraoperative identification of neoplastic tissue and optimizing the extent of resection in primary as well as metastatic brain tumors. 5-ALA positivity in metastatic brain tumors depends on the primary cancer and pathological diagnosis and ranges between 12.5% and 100% [11]. Previous studies reported only clinical or *in vitro* data, whereas this is the first study to investigate

Table 1
Characteristics of ten patients with metastatic brain tumor from NSCLC under 5ALA-guided surgery.

	5-ALA positive	5-ALA negative
Number	n = 5	n = 5
Median age(range)	66(55-78)	58(40-68)
Male : Female	3:2	4:1
Pathological diagnosis		
Squamous Cell Carcinoma	–	1
Adenocarcinoma	3	3
Others[a]	2	1
specimen from lung cancer	3	1

[a] Others ; includes adenosquamous carcinoma, spindle cell carcinoma, giant cell carcinoma.

protoporphyrin IX fluorescence of metastatic brain tumors originating from NSCLC using both *in vitro* sources and clinical specimens. The findings of the current will further the understanding of protoporphyrin IX fluorescence in metastatic brain tumors originating from NSCLC and can potentially lead to more accurate surgical resection.

In a prospective study, Muragaki et al. reported that intraoperative photodynamic therapy using 5-ALA and a semiconductor laser may be considered as a potentially effective and sufficiently safe option for adjuvant management of primary malignant parenchymal brain tumors [24]. Their results as well as the findings of the current study suggest that photodynamic therapy in metastatic brain tumors originating from NSCLC can potentially improve clinical outcomes by upregulating the expression of PEPT1.

4.2. Accumulation of protoporphyrin IX following the administration of 5-ALA in NSCLC cell lines in vitro

The mechanism of protoporphyrin IX accumulation in tumor cells represents a critical issue for successful photodynamic diagnosis and treatment. The present study is the first to report to demonstrate that PEPT1 plays a significant role in the accumulation of protoporphyrin IX in NSCLC cell lines and reveal the mechanism underlying tumor-specific protoporphyrin IX accumulation following 5-ALA administration in NSCLC cells.

A previous study demonstrated that the FECH enzyme is involved in intracellular accumulation of protoporphyrin IX in human glioma cells [14]. Hagiya et al. [21] reported that high PEPT1 expression determined 5-ALA-induced protoporphyrin IX production in gastric cancer. Ishikawa et al. [16] reported that ABCG2 played a critical role in 5-ALA photodynamic diagnosis and therapy in human brain tumors. These results suggest that the key roles of enzymes and transporters in the porphyrin biosynthesis pathway during 5-ALA metabolism vary among tumor types. To the best of our knowledge, only one study reported that a specific ABCG2 inhibitor enhanced the accumulation of protoporphyrin IX in the A549 lung cancer cell line [25]. However, that study investigated only the effects of the ABCG2 inhibitor without evaluating the other enzymes and transporters of the pathway. In the current study, we utilized both western blotting and qRT-PCR to

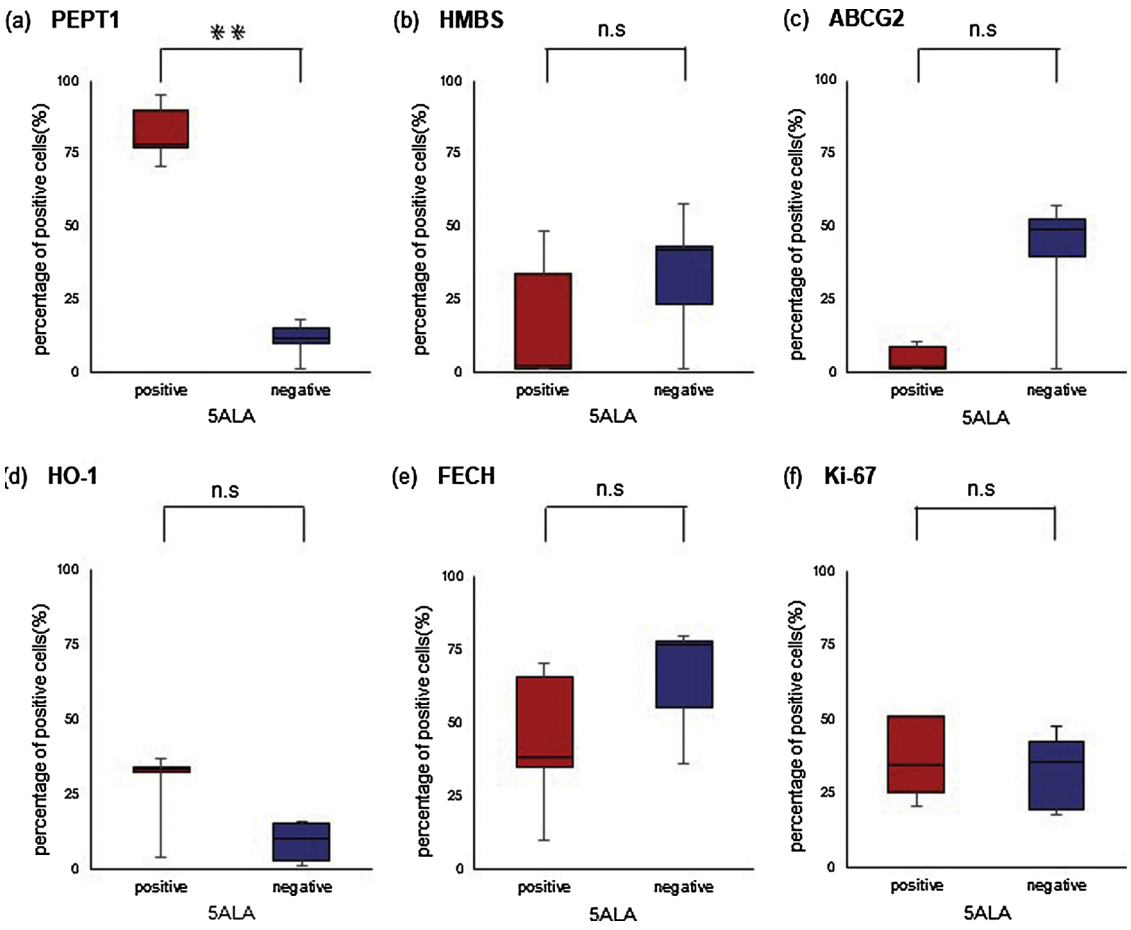

Fig. 4. IHC staining of PEPT1 and intraoperative fluorescence of protoporphyrin IX positive and negative case.
a: H.E staining in fluorescence of protoporphyrin IX positive case. Histology is adenocarcinoma. b: IHC staining of PEPT1 in fluorescence of protoporphyrin IX positive case. c: Intraoperative fluorescence of protoporphyrin IX is positive. d: H.E staining in fluorescence of protoporphyrin IX negative case. Histology is adenocarcinoma. e: HC staining of PEPT1 in fluorescence of protoporphyrin IX negative case. f: Intraoperative fluorescence of protoporphyrin IX is negative.

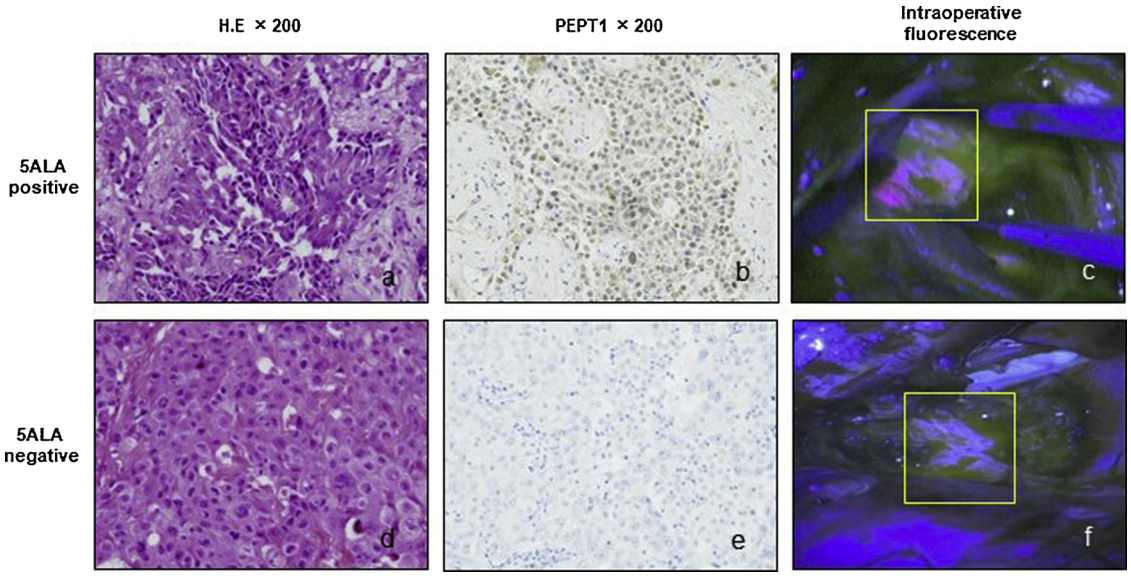

Fig. 5. Correlation between expression of each protein assessed by IHC and protoporphyrin IX fluorescence.
(a)PEPT1: peptide transporter1, (b) HMBS: hydroxymethylbilane synthase, (c) ABCG2: ATP-binding cassette group2, (d) HO-1: heme oxygenase-1, (e) FECH: ferrochelatase, (f) Ki-67

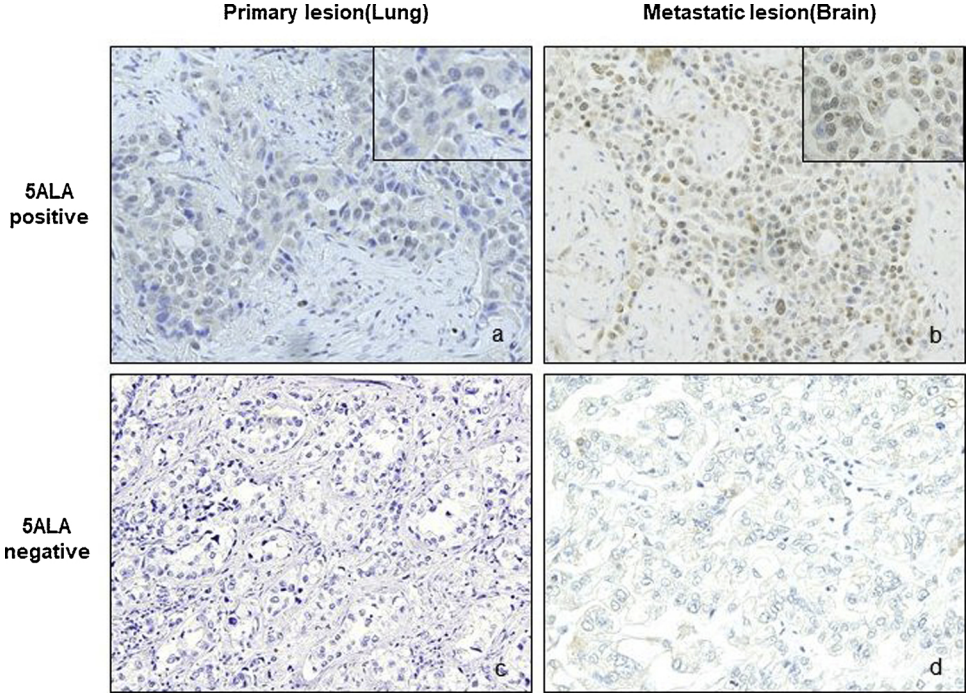

Fig. 6. IHC staining of PEPT1 in primary and metastatic lesion distinguishing in intraoperative fluorescence of protoporphyrin IX positive and negative.
a: IHC staining of PEPT1 of primary lesion in intraoperative fluorescence of protoporphyrin IX positive. b: IHC staining of PEPT1 of metastatic lesion in intraoperative fluorescence of protoporphyrin IX positive. c: IHC staining of PEPT1 of primary lesion in intraoperative fluorescence of protoporphyrin IX negative. d: IHC staining of PEPT1 of metastatic lesion in intraoperative fluorescence of protoporphyrin IX negative.

demonstrate quantitatively that PEPT1 played a significant role in the accumulation of protoporphyrin IX in six NSCLC lines. Our findings implicate that PEPT1 upregulation might enhance the accumulation of protoporphyrin IX in NSCLC cell lines.

4.3. The correlation between quantitative analysis in NSCLC cell lines and immunohistochemistry in clinical samples

This is the first report suggesting that PEPT1 was significantly associated with protoporphyrin IX fluorescence in metastatic brain tumors originating from NSCLC. In the current study, we quantitatively analyzed the protein and mRNA levels in NSCLC cell lines *in vitro*. Additionally, we used immunohistochemistry to evaluate clinical samples harvested from metastatic brain tumors during surgical resection in patients with NSCLC. The comparison of the groups that were positive and negative for protoporphyrin IX fluorescence demonstrated that PEPT1 was a significant factor during 5-ALA-guided surgery. We also compared the PEPT1 levels between the primary (lung) and the metastatic (brain) sites in the same patients using immunohistochemistry. There were no apparent differences in the PEPT1 levels between the primary and metastatic sites. Previous reports suggested that the pathological and molecular nature of the tumor may not be different between the primary and metastatic sites, especially in those expressing epidermal growth factor receptor mutations in lung cancer patients

[26–28]. This was our motivation for evaluating the NSCLC cell lines *in vitro* and metastatic brain tumors originating from lung cancer by immunohistochemistry.

4.4. Limitations

We must acknowledge several limitations of the present study. (1) First, immunohistochemical analysis of the clinical samples showed significant differences, but the number of clinical samples was small. (2) The current study included clinical samples from the primary lung cancer as well as the metastatic site in the brain. The specimens were not harvested simultaneously, which may pose a problem although they were collected from the same patient. The pathological and molecular status of the tumors might have been modified by treatment with chemotherapy and radiotherapy. (3) Further studies are thus necessary to confirm whether siRNA-mediated knockdown of *PEPT1* significantly reduces intracellular accumulation of protoporphyrin IX in NSCLC cell lines and whether NSCLC cells overexpressing PEPT1 using cloning vectors induce intracellular accumulation of protoporphyrin IX *in vitro*.

5. Conclusion

The current study investigating the mechanism of protoporphyrin IX fluorescence in NSCLC and NSCLC-associated metastatic brain tumors revealed that PEPT1 expression was positively correlated with 5-ALA-mediated protoporphyrin IX accumulation in NSCLC cell lines *in vitro* and clinical metastatic brain tumor samples originating from NSCLC. This is the first study to report that PEPT1 plays a significant role in the accumulation of protoporphyrin IX in NSCLC cell lines. Future studies should aim to explore practical methods for overcoming low protoporphyrin IX fluorescence in metastatic brain tumors including upregulation of PEPT1 expression, with subsequent prevention of local recurrence *via* complete tumor resection during 5-ALA-guided surgery.

References

[1] L.M. DeAngelis, Brain tumors, N. Engl. J. Med. 344 (2) (2001) 114–123.
[2] M.A. Kamp, M. Dibue, A. Santacroce, S.M. Zella, L. Niemann, H.J. Steiger, M. Rapp, M. Sabel, The tumour is not enough or is it? Problems and new concepts in the surgery of cerebral metastases, Ecancermedicalscience 7 (2013) 306.
[3] A.S. Berghoff, O. Rajky, F. Winkler, R. Bartsch, J. Furtner, J.A. Hainfellner, S.L. Goodman, M. Weller, J. Schittenhelm, M. Preusser, Invasion patterns in brain metastases of solid cancers, Neuro Oncol. 15 (12) (2013) 1664–1672.
[4] L. Siam, A. Bleckmann, H.N. Chaung, A. Mohr, F. Klemm, A. Barrantes-Freer, R. Blazquez, H.A. Wolff, F. Luke, V. Rohde, C. Stadelmann, T. Pukrop, The metastatic infiltration at the metastasis/brain parenchyma-interface is very heterogeneous and has a significant impact on survival in a prospective study, Oncotarget 6 (30) (2015) 29254–29267.
[5] W. Stummer, U. Pichlmeier, T. Meinel, O.D. Wiestler, F. Zanella, H.J. Reulen, A.L.-G.S. Group, Fluorescence-guided surgery with 5-aminolevulinic acid for resection of malignant glioma: a randomised controlled multicentre phase III trial, Lancet Oncol. 7 (5) (2006) 392–401.
[6] K. Inoue, H. Fukuhara, T. Shimamoto, M. Kamada, T. Iiyama, M. Miyamura, A. Kurabayashi, M. Furihata, M. Tanimura, H. Watanabe, T. Shuin, Comparison between intravesical and oral administration of 5-aminolevulinic acid in the clinical benefit of photodynamic diagnosis for nonmuscle invasive bladder cancer, Cancer 118 (4) (2012) 1062–1074.
[7] M.A. Kamp, P. Grosser, J. Felsberg, P.J. Slotty, H.J. Steiger, G. Reifenberger, M. Sabel, 5-aminolevulinic acid (5-ALA)-induced fluorescence in intracerebral metastases: a retrospective study, Acta Neurochir. (Wien) 154 (2) (2012) 223–228 discussion 228.
[8] J.C. Kennedy, R.H. Pottier, Endogenous protoporphyrin IX, a clinically useful photosensitizer for photodynamic therapy, J. Photochem. Photobiol. B 14 (4) (1992) 275–292.
[9] L. Gossner, M. Stolte, R. Sroka, K. Rick, A. May, E.G. Hahn, C. Ell, Photodynamic ablation of high-grade dysplasia and early cancer in Barrett's esophagus by means of 5-aminolevulinic acid, Gastroenterology 114 (3) (1998) 448–455.
[10] Q. Peng, T. Warloe, K. Berg, J. Moan, M. Kongshaug, K.E. Giercksky, J.M. Nesland, 5-Aminolevulinic acid-based photodynamic therapy. Clinical research and future challenges, Cancer 79 (12) (1997) 2282–2308.
[11] S. Marbacher, E. Klinger, L. Schwyzer, I. Fischer, E. Nevzati, M. Diepers, U. Roelcke, A.R. Fathi, D. Coluccia, J. Fandino, Use of fluorescence to guide resection or biopsy of primary brain tumors and brain metastases, Neurosurg. Focus 36 (2) (2014) E10.
[12] M.A. Kamp, I. Fischer, J. Buhner, B. Turowski, J.F. Cornelius, H.J. Steiger, M. Rapp, P.J. Slotty, M. Sabel, 5-ALA fluorescence of cerebral metastases and its impact for the local-in-brain progression, Oncotarget 7 (41) (2016) 66776–66789.
[13] M. Millesi, B. Kiesel, M. Mischkulnig, M. Martinez-Moreno, A. Wohrer, S. Wolfsberger, E. Knosp, G. Widhalm, Analysis of the surgical benefits of 5-ALA-induced fluorescence in intracranial meningiomas: experience in 204 meningiomas, J. Neurosurg. 125 (6) (2016) 1408–1419.
[14] L. Teng, M. Nakada, S.G. Zhao, Y. Endo, N. Furuyama, E. Nambu, I.V. Pyko, Y. Hayashi, J.I. Hamada, Silencing of ferrochelatase enhances 5-aminolevulinic acid-based fluorescence and photodynamic therapy efficacy, Br. J. Cancer 104 (5) (2011) 798–807.
[15] S.G. Zhao, X.F. Chen, L.G. Wang, G. Yang, D.Y. Han, L. Teng, M.C. Yang, D.Y. Wang, C. Shi, Y.H. Liu, B.J. Zheng, C.B. Shi, X. Gao, N.G. Rainov, Increased expression of ABCB6 enhances protoporphyrin IX accumulation and photodynamic effect in human glioma, Ann. Surg. Oncol. 20 (13) (2013) 4379–4388.
[16] T. Ishikawa, Y. Kajimoto, Y. Inoue, Y. Ikegami, T. Kuroiwa, Critical role of ABCG2 in ALA-photodynamic diagnosis and therapy of human brain tumor, Adv. Cancer Res. 125 (2015) 197–216.
[17] M. Hayashi, H. Fukuhara, K. Inoue, T. Shuin, Y. Hagiya, M. Nakajima, T. Tanaka, S. Ogura, The effect of iron ion on the specificity of photodynamic therapy with 5-aminolevulinic acid, PLoS One 10 (3) (2015) e0122351.
[18] W. Wang, K. Tabu, Y. Hagiya, Y. Sugiyama, Y. Kokubu, Y. Murota, S.I. Ogura, T. Taga, Enhancement of 5-aminolevulinic acid-based fluorescence detection of side population-defined glioma stem cells by iron chelation, Sci. Rep. 7 (2017) 42070.
[19] M. Ishizuka, F. Abe, Y. Sano, K. Takahashi, K. Inoue, M. Nakajima, T. Kohda, N. Komatsu, S. Ogura, T. Tanaka, Novel development of 5-aminolevurinic acid (ALA) in cancer diagnoses and therapy, Int. Immunopharmacol. 11 (3) (2011) 358–365.
[20] Y. Hagiya, Y. Endo, Y. Yonemura, K. Takahashi, M. Ishizuka, F. Abe, T. Tanaka, I. Okura, M. Nakajima, T. Ishikawa, S. Ogura, Pivotal roles of peptide transporter PEPT1 and ATP-binding cassette (ABC) transporter ABCG2 in 5-aminolevulinic acid (ALA)-based photocytotoxicity of gastric cancer cells in vitro, Photodiagnosis Photodyn. Ther. 9 (3) (2012) 204–214.
[21] Y. Hagiya, H. Fukuhara, K. Matsumoto, Y. Endo, M. Nakajima, T. Tanaka, I. Okura, A. Kurabayashi, M. Furihata, K. Inoue, T. Shuin, S. Ogura, Expression levels of PEPT1 and ABCG2 play key roles in 5-aminolevulinic acid (ALA)-induced tumor-specific protoporphyrin IX (PpIX) accumulation in bladder cancer, Photodiagnosis Photodyn. Ther. 10 (3) (2013) 288–295.
[22] M. Miyake, M. Ishii, K. Kawashima, T. Kodama, K. Sugano, K. Fujimoto, Y. Hirao, siRNA-mediated knockdown of the heme synthesis and degradation pathways: modulation of treatment effect of 5-aminolevulinic acid-based photodynamic therapy in urothelial cancer cell lines, Photochem. Photobiol. 85 (4) (2009) 1020–1027.
[23] Y. Nakai, Y. Tatsumi, M. Miyake, S. Anai, M. Kuwada, S. Onishi, Y. Chihara, N. Tanaka, Y. Hirao, K. Fujimoto, Expression of ferrochelatase has a strong correlation in protoporphyrin IX accumulation with photodynamic detection of bladder cancer, Photodiagnosis Photodyn. Ther. 13 (2016) 225–232.
[24] Y. Muragaki, J. Akimoto, T. Maruyama, H. Iseki, S. Ikuta, M. Nitta, K. Maebayashi, T. Saito, Y. Okada, S. Kaneko, A. Matsumura, T. Kuroiwa, K. Karasawa, Y. Nakazato, T. Kayama, Phase II clinical study on intraoperative photodynamic therapy with talaporfin sodium and semiconductor laser in patients with malignant brain tumors, J. Neurosurg. 119 (4) (2013) 845–852.
[25] H. Fujita, K. Nagakawa, H. Kobuchi, T. Ogino, Y. Kondo, K. Inoue, T. Shuin, T. Utsumi, K. Utsumi, J. Sasaki, H. Ohuchi, Phytoestrogen suppresses efflux of the diagnostic marker protoporphyrin IX in lung carcinoma, Cancer Res. 76 (7) (2016) 1837–1846.
[26] Y. Yatabe, K. Matsuo, T. Mitsudomi, Heterogeneous distribution of EGFR mutations is extremely rare in lung adenocarcinoma, J. Clin. Oncol. 29 (22) (2011) 2972–2977.
[27] F. Zito Marino, G. Liguori, G. Aquino, E. La Mantia, S. Bosari, S. Ferrero, L. Rosso, G. Gaudioso, N. De Rosa, M. Scrima, N. Martucci, A. La Rocca, N. Normanno, A. Morabito, G. Rocco, G. Botti, R. Franco, Intratumor heterogeneity of ALK-Rearrangements and homogeneity of EGFR-Mutations in mixed lung adenocarcinoma, PLoS One 10 (9) (2015) e0139264.
[28] K. Suda, I. Murakami, H. Yu, K. Ellison, M. Shimoji, C. Genova, C.J. Rivard, T. Mitsudomi, F.R. Hirsch, Heterogeneity of EGFR aberrations and correlation with histological structures: analyses of therapy-naive isogenic lung Cancer lesions with EGFR mutation, J. Thorac. Oncol. 11 (10) (2016) 1711–1717.